



## Slip Flow Effects over Hydromagnetic Forced Convective Flow over a Slendering Stretching Sheet

S. P. Anjali Devi and M. Prakash †

*Department of Applied Mathematics, Bharathiar University, Coimbatore, Tamil Nadu, 641 046, India*

† Corresponding Author Email: [prakash\\_fluidmech@outlook.com](mailto:prakash_fluidmech@outlook.com)

(Received September 17, 2014; accepted November 19, 2014)

### ABSTRACT

The objective of this study is to determine the characteristics of hydromagnetic flow over a slendering stretching sheet in slip flow regime. Steady, two dimensional, nonlinear, hydromagnetic laminar flow of an incompressible, viscous and electrically conducting fluid over a stretching sheet with variable thickness in the presence of variable magnetic field and slip flow regime is considered. Governing equations of the problem are converted into ordinary differential equations utilizing similarity transformations. The resulting non-linear differential equations are solved numerically by utilizing Nachtsheim-swigert shooting iterative scheme for satisfaction of asymptotic boundary conditions along with fourth order Runge-Kutta integration method. Numerical computations are carried out for various values of the physical parameters and their effects over the velocity and temperature are analyzed. Numerical values of dimensionless skin friction coefficient and non-dimensional rate of heat transfer are also obtained.

**Keywords:** Variable thickness, Stretching sheet, Magneto hydrodynamics, Slip flow.

### NOMENCLATURE

$A$	coefficient related to stretching sheet	$Re_x$	local Reynolds number
$a$	thermal accommodation coefficient	$T$	fluid temperature
$b$	physical parameter related to stretching sheet	$T_w(x)$	wall temperature
$C_p$	specific heat at constant pressure	$T_\infty$	temperature far away from the sheet
$f_1$	maxwell's reflection coefficient	$u$	velocity component in the $x$ directions
$h_1^*$	dimensional velocity slip parameter	$v$	velocity component in the $y$ directions
$h_2^*$	dimensional temperature jump parameter	$\gamma$	ratio of specific heats
$h_1$	dimensionless velocity slip parameter	$\eta$	plate surface
$h_2$	dimensionless temperature jump parameter	$\lambda$	wall thickness parameter
$k$	thermal conductivity of the fluid	$\nu$	kinematic viscosity
$M^2$	magnetic interaction parameter	$\rho$	density of the fluid
$m$	velocity power index parameter	$\sigma$	electrical conductivity of the fluid
$Pr$	Prandtl number	$\xi_1$	mean free path (Constant)

### 1. INTRODUCTION

Recent years have seen rapid advancement in medical and technological research fields especially in the area of medical device production and miniature technology. In spite of their precautionary procedures in the manufacturing of

cardiac rhythm management devices like artificial pacemaker, the electromagnetic interface remains as a real concern and potential danger Sweesy *et al.* (2004). The smoothening thickness of such artificial devices, artificial heart valves, internal cavities, and micro/nano -electronic mechanical systems is vi-

tal and which are characterized by slip flows over variable thickness sheets. Due to their smaller size those micro devices may get heated quickly. In those situations the suitable heat transfer techniques are needed. For future medical research regarding these physical phenomena, the combined knowledge of MHD flows and heat transfer over with varying thickness sheet and slip flow regime are essential. Research on boundary layer flow over a stretching sheet has become desire and attracted much attention because of its ever growing industrial applications. In most of the traditional boundary layer flow problems over the stretching sheet, they consider the sheet to be flat. Practically, the stretching sheet need not be flat. Sheet with variable thickness can be encountered more often in real world applications. The boundary layer flow over a stretching sheet with variable thickness has received great attention in recent years owing to its abundant practical applications in machine design, architecture, nuclear reactor technology, naval structures, acoustical components, chemical and manufacturing processes, such as polymer extrusion, hot rolling, spinning of filaments, metal extrusion, crystal growing, glass fiber production, paper production, continuous casting of metals, copper wires drawing and glass blowing Altan *et al.* (1979), Fisherl (1976) and Karwe and Jaluria (1991). Motivated by these applications this work is mainly focused to analyze the influence of these physical phenomena through the physical parameters.

Flow of an electrically conducting fluid over a stretching sheet along with heat transfer has gained considerable attention due to its vast applications in the industry and important bearings on several technological and natural processes. Examples include the boundary layer control in the field of aerodynamics, cooling of nuclear reactors, cooling of a metallic plate in a cooling bath, geothermal energy extraction, operation of magnetohydrodynamic (MHD) generators, plasma studies, etc. Some research contributions towards this field is found below. Sparrow and Cess (1961) reported the effect of magnetic field on the natural convection heat transfer. Chakrabarti and Gupta (1979) analyzed the hydromagnetic flow and heat transfer over a stretching sheet. Behrouz *et al.* (2011) obtained the solution to the MHD flow over a non-linear stretching sheet.

The flow in micro/nano systems such as hard disk drive, micro-pump, micro-valve and micro-nozzles is in slip transition regime, which is characterized by slip boundary at the wall. The

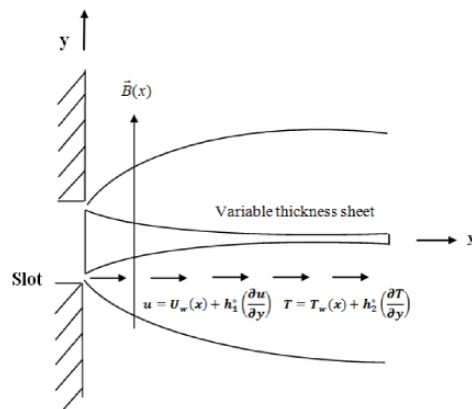


**Fig. 1. Schematic diagram of the problem.**

liquids exhibiting boundary slip find its applications in technological problems. Therefore many boundary layer fluid flow problems have been revisited with slip boundary condition and different researchers have made significant contributions. Navier (1827) suggested a slip boundary condition in terms of shear stress. Of late, the work of Navier was extended by many authors. GadelHak (1999) established the fact that the micro-scale level the fluid flow is dominated by fluid surface interaction which belongs to slip flows regime, whereas the momentum equation remains to be Navier-Stokes equation. Slip flow past a stretching surface was analyzed by Andersson (2002). Wang (2009) attempted an analysis of viscous flow due to a stretching sheet with surface slip and suction. Dissipation effects on MHD nonlinear flow and heat transfer past a porous surface with prescribed heat flux was studied by Anjali and Ganga (2010). Yazdi *et al.* (2011) analyzed the Slip MHD liquid flow and heat transfer over non-linear permeable stretching surface. Slip effects on MHD boundary layer flow over an exponentially stretching sheet with suction/blowing and thermal radiation was reported by Mukhopadhyay (2013).

Practically, the stretching sheet need not be flat. Sheet with variable thickness can be encountered more often in real world applications. Plates with variable thickness are often used in machine design, architecture, nuclear reactor technology, naval structures and acoustical components. Variable thickness is one of the significant properties in the analysis of vibration of orthotropic plates. Historically the concepts of variable thickness sheets originate through linearly deforming substance such as needles and nozzles. Idea about the variable thickness sheet was initiated by Lee (1967) through thin needles. Later, Fang *et al.* (2012) analyzed the

behavior of boundary layer flow over a stretching sheet with variable thickness. The numerical solution for boundary layer flow due to a nonlinearly stretching sheet with variable thickness and slip velocity has been obtained by Khader and Megahed (2013). Recently, Anjali and Prakash (2014) studied the hydromagnetic flow over a stretching sheet with variable thickness and variable surface temperature.

So far no attempt has been tried towards hydro-magnetic boundary layer flow and heat transfer over a stretching sheet with variable thickness in slip flow regime. In this work, a special form of magnetic field, velocity slip and temperature jump are considered to analyze the various aspects of the flow and heat transfer effects.

**2. FORMULATION OF THE PROBLEM**

Steady, two dimensional, nonlinear, laminar hydromagnetic flow of an incompressible, viscous and electrically conducting fluid over a stretching sheet with variable thickness in slip flow regime is considered. The  $x$ -axis is chosen in the direction of the sheet motion and the  $y$ -axis is perpendicular to it.

The following assumptions are made

- The sheet is stretching with the velocity  $U_w(x) = U_0(x+b)^m$  and the wall is impermeable with  $v_w = 0$ .
- The sheet is not flat described as  $y = A(x+b)^{\frac{1-m}{2}}$  and the coefficient  $A$  is chosen as small for the sheet to be sufficiently thin, to avoid pressure gradient along the sheet ( $\frac{\partial p}{\partial x} = 0$ ).
- The magnetic Reynolds number is assumed as so small so that the induced magnetic field is negligible. As the induced magnetic field is assumed to be negligible and since  $B(x)$  is independent of time,  $curl \vec{E} = 0$ . In the absence of surface charge density,  $div \vec{E} = 0$ . Hence the external electric field is assumed as negligible.
- The problem is valid for  $m \neq 1$  since  $m = 1$  refers to the flat sheet case.
- The viscous and Joule dissipation are considered to be negligible.

Under the above assumptions, the steady boundary layer equations are given by Anjali Devi and Thiyagarajan (2006)

$$\frac{\partial u}{\partial x} + v \frac{\partial v}{\partial y} = 0, \tag{1}$$

$$u \frac{\partial u}{\partial x} + v \frac{\partial u}{\partial y} = \nu \frac{\partial^2 u}{\partial y^2} - \frac{\sigma B(x)^2 u}{\rho}, \tag{2}$$

$$u \frac{\partial T}{\partial x} + v \frac{\partial T}{\partial y} = \frac{k}{\rho C_p} \frac{\partial^2 T}{\partial y^2} \tag{3}$$

with the boundary conditions

$$\begin{cases} u(x, A(x+b)^{\frac{1-m}{2}}) = U_w(x) + h_1^* \left( \frac{\partial u}{\partial y} \right) \\ \qquad \qquad \qquad = U_0(x+b)^m + h_1^* \left( \frac{\partial u}{\partial y} \right), \\ v(x, A(x+b)^{\frac{1-m}{2}}) = 0, \\ T(x, A(x+b)^{\frac{1-m}{2}}) = T_w(x) + h_2^* \left( \frac{\partial T}{\partial y} \right), \\ u(x, \infty) = 0, T(x, \infty) = T_\infty, (m \neq 1), \end{cases} \tag{4}$$

where

$$h_1^* = \left[ \frac{2-f_1}{f_1} \right] \xi_1 (x+b)^{\frac{1-m}{2}}, \tag{5}$$

$$h_2^* = \left[ \frac{2-a}{a} \right] \xi_2 (x+b)^{\frac{1-m}{2}}, \xi_2 = \left( \frac{2\gamma}{\gamma+1} \right) \frac{\xi_1}{Pr}. \tag{6}$$

**3. SIMILARITY TRANSFORMATIONS**

The special form of magnetic field and wall temperature are taken as

$$B(x) = B_0 (x+b)^{\frac{m-1}{2}}, (m \neq 1), \tag{7}$$

and

$$T_w(x) = T_\infty + T_0 (x+b)^{\frac{1-m}{2}}, (m \neq 1). \tag{8}$$

The above forms are considered to obtain the similarity solutions. In order to solve the Eq. 1 - Eq. 3 subject to Eq. 2., the stream function and similarity transformations are introduced as follows:

$$\psi(x,y) = f(\eta) \sqrt{\frac{2}{m+1}} \nu U_0 (x+b)^{m+1}, (m \neq 1) \tag{9}$$

$$\eta = y \sqrt{\frac{m+1}{2} \frac{U_0 (x+b)^{m-1}}{\nu}}, (m \neq 1), \tag{10}$$

$$\theta = \frac{T - T_\infty}{T_w(x) - T_\infty}. \tag{11}$$

For the validity of the similarity variable and functions, it is assumed  $m > -1$  in this work. Eqns. 3 - 11 are proposed based on the standard practice for similarity transformation of partial differential equations. The stream function  $\psi$  is defined as

$$u = \frac{\partial \psi}{\partial y} \quad \text{and} \quad v = -\frac{\partial \psi}{\partial x}. \tag{12}$$

Using the Eq. 3., Eq. 10 and Eq. 12, the velocity components are expressed as follows

$$u = U_0 (x+b)^m f'(\eta), (m \neq 1), \tag{13}$$

$$v = -\sqrt{\frac{m+1}{2}} v U_0 (x+b)^{m-1}$$

$$\left[ f'(\eta) \eta \left( \frac{m-1}{m+1} \right) + f(\eta) \right], (m \neq 1). \tag{14}$$

Equation of continuity Eq. 1 is automatically satisfied. Using the similarity transformations Eq. 7 - Eq. 11, the nonlinear partial differential equations Eq. 2 and Eq. 3 with boundary conditions Eq. 2. are reduced to the following nonlinear ordinary differential equations:

$$f''' = \left[ \left( \frac{2m}{m+1} \right) (f')^2 - f f'' + M^2 f' \right], \tag{15}$$

$$\theta'' = Pr \left[ \left( \frac{1-m}{m+1} \right) f' \theta - f \theta' \right] \tag{16}$$

with the boundary conditions

$$\left\{ \begin{array}{l} f(\lambda) = \lambda \left( \frac{1-m}{m+1} \right) [1 + h_1 f''(0)], \\ f'(\lambda) = [1 + h_1 f''(0)], \\ \theta(\lambda) = [1 + h_2 \theta'(0)], \\ f'(\infty) = 0, \theta(\infty) = 0, (m \neq 1), \end{array} \right. \tag{17}$$

where  $\lambda = A \sqrt{\frac{m+1}{2}} \frac{U_0}{v}$ ,

$$h_1 = \left[ \frac{2-f_1}{f_1} \right] \xi_1 \sqrt{\frac{U_o(m+1)}{2v}} \text{ and}$$

$$h_2 = \left[ \frac{2-a}{a} \right] \xi_2 \sqrt{\frac{U_o(m+1)}{2v}}.$$

**Table 1 Numerical values of  $-F''(0)$  when  $M^2 = 0, h_2 = 0$  and  $m = 0.5$**

$h_1$	$\lambda$	Khader and Megahed (2013)	Present work
0.0	0.2	0.924828	0.9248281
0.2	0.25	0.733395	0.7333949
0.2	0.5	0.759570	0.7595701

Eq. 15 and Eq. 16 with the boundary conditions Eq. 17 are the nonlinear differential equations with a domain  $[\lambda, \infty)$ . In order to facilitate the computation and to transform the domain into  $[0, \infty)$ , we define  $F(\xi) = F(\eta - \lambda) = f(\eta)$ . The similarity equations become

$$F''' = \left[ \left( \frac{2m}{m+1} \right) (F')^2 - F F'' + M^2 F' \right], \tag{18}$$

$$\Theta'' = Pr \left[ \left( \frac{1-m}{m+1} \right) F' \Theta - F \Theta' \right] \tag{19}$$

with the boundary conditions

$$\left\{ \begin{array}{l} F(0) = \lambda \left( \frac{1-m}{m+1} \right) [1 + h_1 F''(0)], \\ F'(0) = [1 + h_1 F''(0)], \\ \Theta(0) = [1 + h_2 \Theta'(0)], \\ F'(\infty) = 0, \Theta(\infty) = 0, (m \neq 1), \end{array} \right. \tag{20}$$

where the prime indicates differentiation with respect to  $\xi$ ,  $M^2 = \frac{2\sigma B_0^2}{\rho U_0(m+1)}$ ,  $Pr = \frac{\mu C_p}{k}$ . Based on the variable transformation, the solution domain will be fixed from 0 to  $\infty$ .

The important physical quantities of interest, the skin-friction coefficient  $C_f$  and local Nusselt number  $Nu_x$  are defined as

$$\left. \begin{array}{l} C_f = \frac{\mu \left( \frac{\partial u}{\partial y} \right)_{y=A(x+b) \frac{1-m}{2}}}{\frac{1}{2} \rho U_w^2} \\ = 2 \sqrt{\frac{m+1}{2}} (Re_x)^{-\frac{1}{2}} F''(0), \end{array} \right\} \tag{21}$$

$$\left. \begin{array}{l} Nu_x = \frac{(x+b) \left( \frac{\partial T}{\partial y} \right)_{y=A(x+b) \frac{1-m}{2}}}{(T_w(x) - T_\infty)} \\ = -\sqrt{\frac{m+1}{2}} (Re_x)^{\frac{1}{2}} \Theta'(0), \end{array} \right\} \tag{22}$$

where  $Re_x = \frac{U_w X}{v}$  and  $X = (x+b)$ .

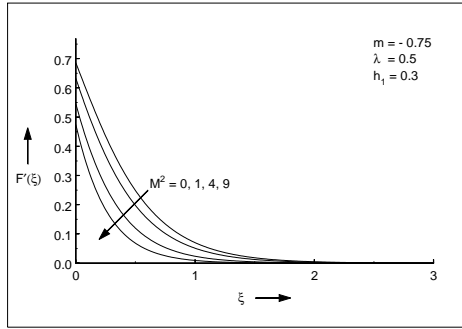


**Fig. 2. Velocity distribution for various values of  $M^2$ .**

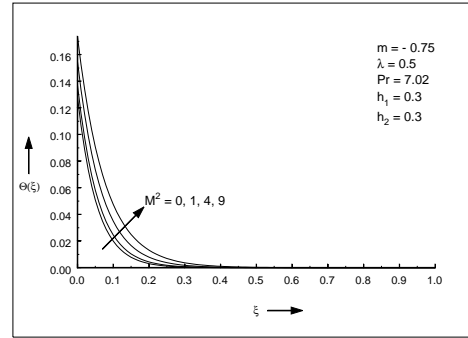


**Fig. 3. Temperature distribution for various values of  $M^2$ .**

#### 4. NUMERICAL SOLUTION

An efficient Nachtsheim-Swigert shooting iteration technique Nachtsheim and Swigert (1965) for the satisfaction of the asymptotic boundary conditions along with fourth order RungeKutta method has been employed to study the flow model for the above non-linear ordinary differential Eq. 18 and Eq. 19 for different values of governing physical parameters over the flow field and dimensionless temperature distribution. The governing system of partial differential equations are first reduced to a system of ordinary differential equations. The crux of the problem is that we have to make an initial guess for the values of  $F''(0)$  and  $\Theta'(0)$ . The different initial guesses were made are taken into account of the convergence. The process is repeated until the results are corrected upto desired accuracy of  $10^{-5}$  level. Numerical values of dimensionless skin friction coefficient and non dimensional rate of heat transfer are also obtained.

#### 5. RESULTS AND DISCUSSION

The ultimate goal of this work is to establish the influence of magnetic field and other physical parameters over the stretching sheet with variable thickness in the slip flow regime. The reliability of the numerical procedure of this work has been tested through the comparison analysis. In the absence of magnetic interaction parameter ( $M^2 = 0$ ) and nondimensional temperature jump parameter ( $h_2 = 0$ ), the numerical values of  $-F''(0)$  are found to be in excellent agreement with that of Khader and Megahed (2013) which are displayed in Table 1.

The numerical analysis has been carried out for various values of  $M^2$  ( $0 \leq M^2 \leq 9$ ),  $m$  ( $-0.9 \leq m \leq 0.5$ ),  $\lambda$  ( $0.25 \leq \lambda \leq 1.25$ ),  $h_1$  ( $0.0 \leq h_1 \leq 0.7$ ),  $h_2$  ( $0.0 \leq h_2 \leq 0.7$ ) and  $Pr$  ( $0.71 \leq Pr \leq 7.02$ ). In order to get the clear insight of the problem, the computed results are

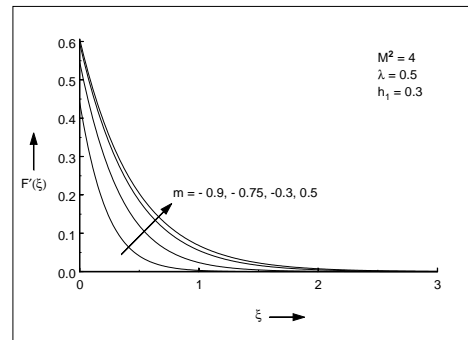


**Fig. 4. Velocity distribution for various values of  $m$ .**

displayed graphically through Fig. 2. - Fig. 16.

The velocity distribution for different values of  $M^2$  was elucidated through Fig. 2. As the magnetic interaction parameter ( $M^2$ ) increases, the velocity distribution and the boundary layer thickness gets decreased. This happens due to Lorentz force arising from the interaction of magnetic and electric fields during the motion of an electrically conducting fluid. The generated Lorentz force opposes the fluid motion in boundary layer region and thereby reducing the momentum boundary layer thickness.

Fig. 3. portrays the influence of magnetic field over dimensionless temperature distribution. It is noted that, the increase in the value of magnetic interaction parameter ( $M^2$ ) leads to increase in the temperature distribution. Since the Lorentz force tends to suppress the flow motion for increasing magnetic field strength, the tendency of the flow to drive away the temperature from the sheet is reduced and consequently makes the heat transfer process slower. This essentially causes the enhancement in thermal boundary layer thickness for increasing strength of the magnetic field.

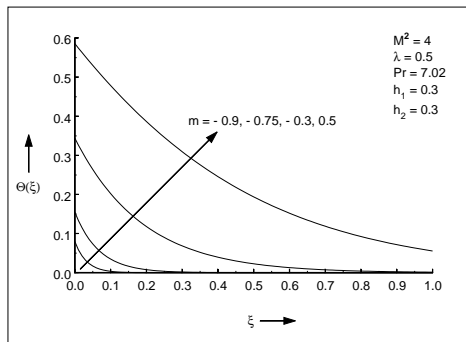


**Fig. 5. Temperature distribution for various values of  $m$ .**

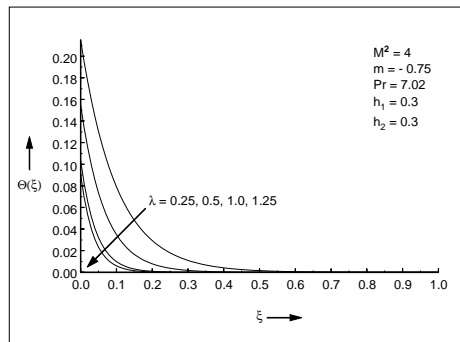


**Fig. 7. Temperature distribution for various values of  $\lambda$ .**

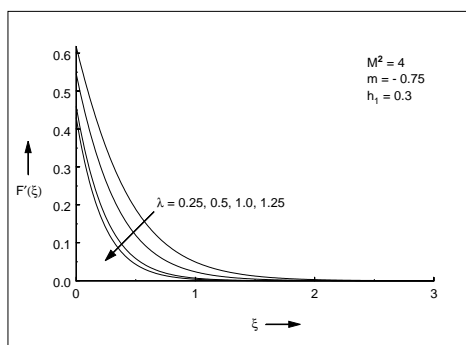


**Fig. 6. Velocity distribution for various values of  $\lambda$ .**

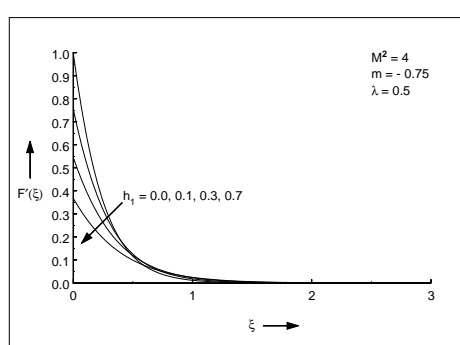


**Fig. 8. Velocity distribution for various values of  $h_1$ .**

Velocity distribution for different values of velocity power index is visualized through Fig. 4. It shows that, due to the fact that increase in velocity power index parameter ( $m$ ) leads to the slenderness of the stretching sheet. As the thickness of the sheet gets reduced, the flow velocity gets accelerated in such slenderness regions so the velocity distribution gets increased. Eventually the boundary layer thickness gets thicker as the velocity power index increase.

Fig. 5. reveals the effect of velocity power index over the temperature distribution. Practically it is known that the heat transfer from thinner region will be greater than that of thicker region. Hence due to increase in velocity power index ( $m$ ), the thickness of the sheet gets reduced which leads to enhancement in the temperature distribution. Significantly the thermal boundary layer gets thicker for larger values of velocity power index.

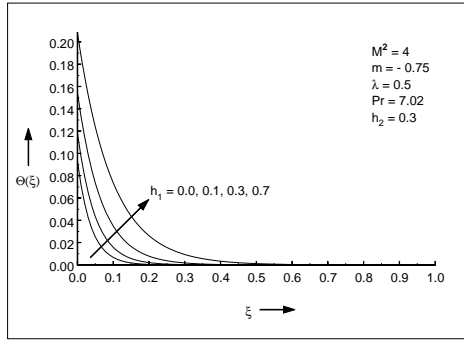
The variation in velocity distribution and temperature distribution due to increase in wall thickness parameter ( $\lambda$ ) were depicted through Fig. 6. and Fig. 7. respectively. The wall thickness decrease for the variable thickness sheet slenderness away from the slot, as it is stretch-

ing away. Increasing values of wall thickness parameter reduces the boundary layer thickness due to decreasing velocity which is illustrated in Fig. 6.

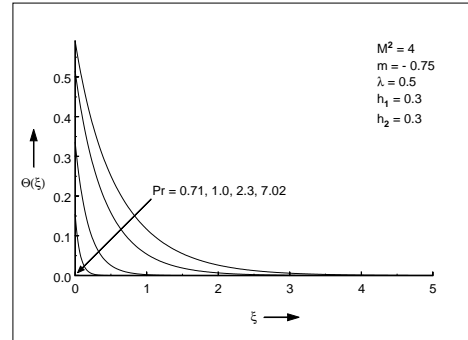
It is evident through Fig. 7. that increase in wall thickness parameter is to reduce the temperature distribution. The thermal boundary layer becomes thinner for higher values of wall thickness parameter.

Fig. 8. shows the effect of dimensionless velocity slip parameter over the velocity distribution. It is inferred from the figure that the presence of slip velocity within the boundary layer causes the velocity level along the sheet to decrease. Initially, for the increasing values of the slip parameter the velocity distribution gets decreased near the surface of the sheet since not all the pulling force of the stretching sheet can be transmitted to the fluid but it gets increased away from the sheet. Due to that greater separation from the sheet, the wall slip factor exerts progressively diminishing influence favours the reversed effect.

Variation in dimensionless temperature distribution due to dimensionless velocity slip pa-



**Fig. 9.** Temperature distribution for various values of  $h_1$ .



**Fig. 11.** Temperature distribution for various values of  $Pr$ .

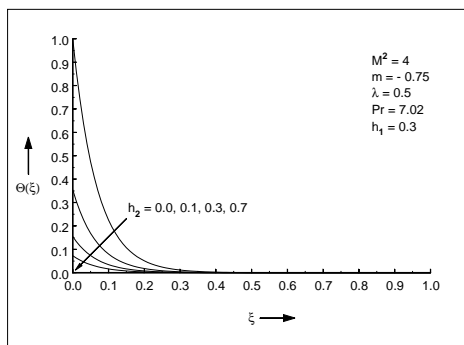


**Fig. 10.** Temperature distribution for various values of  $h_2$ .

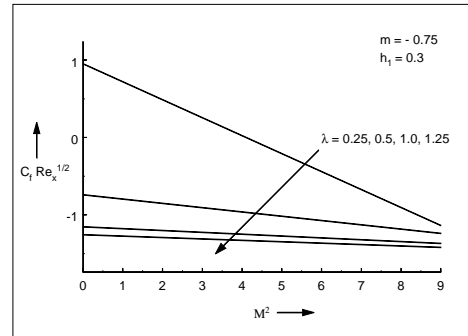


**Fig.12.** Non dimensional skin friction coefficient against  $M^2$  for different values of  $\lambda$ .

parameter is presented graphically in Fig. 9. It shows that increase in the dimensionless velocity slip parameter enhances the dimensionless temperature and thermal boundary layer thickness. Physically, flow velocity is significant to drive out the temperature from the sheet. Near the sheet, the dimensionless velocity slip parameter reduces the flow velocity which leads to increase in dimensionless temperature and simultaneously the thermal boundary layer thickness.

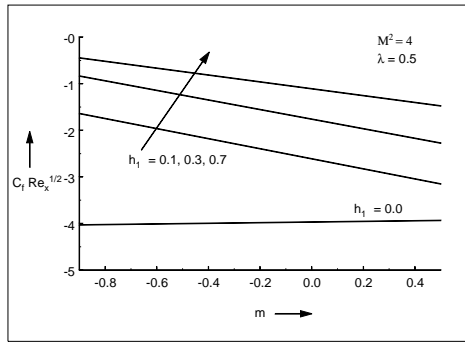
Fig. 10. highlights the impact of dimensionless temperature jump parameter over the dimensionless temperature distribution. It is evident an obvious result that, the dimensionless temperature gets decreased for increasing values of dimensionless temperature jump parameter. Since the increase in temperature jump parameter, increases the thermal accommodation coefficient which reduces the thermal diffusion towards the flow. The thermal boundary layer also gets thinner due to increase in dimensionless temperature jump parameter.

Dimensionless temperature distribution for various values of Prandtl number is displayed

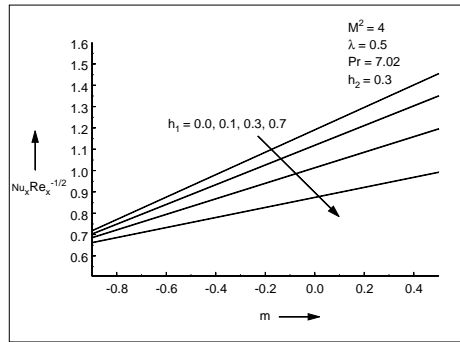
through Fig. 11. It reveals that, eventually both the dimensionless temperature distribution and thermal boundary layer thickness gets decreased due to the slow rate of thermal diffusion which is induced by the increasing values of Prandtl number.

Fig. 12. and Fig. 13. represents the influence of various physical parameters like Magnetic interaction parameter ( $M^2$ ), Velocity power index ( $m$ ), wall thickness parameter ( $\lambda$ ) and dimensionless velocity slip parameter ( $h_1$ ) over the dimensionless skin friction coefficient. Non dimensional skin friction coefficient against magnetic interaction parameter ( $M^2$ ) for different values of wall thickness parameter ( $\lambda$ ) is presented in Fig. 12. It shows that the dimensionless skin friction coefficient decreases for both increased values of magnetic interaction parameter and wall thickness parameter.

The effect of different values of dimensionless velocity slip parameter over the dimensionless skin friction coefficient against velocity power index parameter can be viewed through Fig. 13. It portrays an interesting result for the no-slip case ( $h_1 = 0$ ), the increase in the velocity power



**Fig. 13.** Non dimensional skin friction coefficient against  $m$  for different values of  $h_1$ .



**Fig. 15.** Non dimensional rate of heat transfer against  $m$  for different values of  $h_1$ .

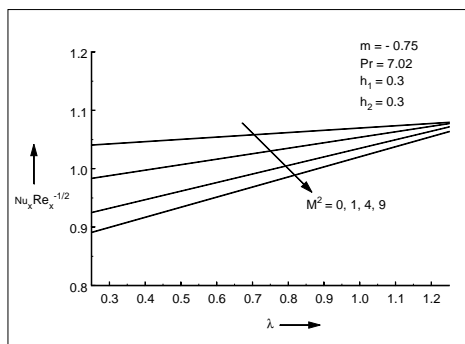


**Fig. 14.** Non dimensional rate of heat transfer against  $\lambda$  for different values of  $M^2$ .

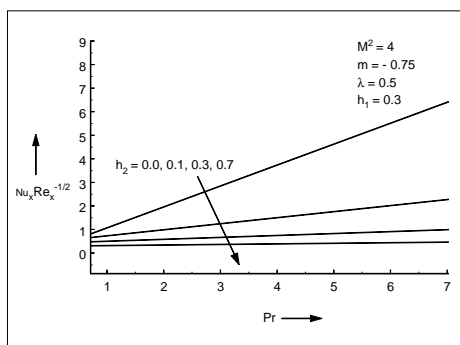


**Fig. 16.** Non dimensional rate of heat transfer against  $Pr$  for different values of  $h_2$ .

index parameter increased the skin friction coefficient, whereas for velocity slip  $h_1 > 0$ , the skin friction coefficient gets decreased for increasing values of velocity power index parameter. It is also noted that, for increasing values of dimensionless velocity slip parameter, the nondimensional skin friction coefficient gets increased.

Fig. 14. elucidates the non dimensional rate of heat transfer against wall thickness parameter ( $\lambda$ ) for various values of magnetic interaction parameter ( $M^2$ ). The magnetic interaction parameter suppress the non dimensional rate of heat transfer as it increases, whereas the wall thickness parameter is to enhance the non dimensional heat transfer rate. Variation in the non dimensional rate of heat transfer against velocity power index parameter ( $m$ ) for different values of dimensionless velocity slip parameter ( $h_1$ ) were depicted through Fig. 15. It is observed that the increase in the dimensionless velocity slip parameter reduces the non dimensional rate of heat transfer whereas the velocity power index parameter has the tenancy to enhance the nondimensional rate of heat transfer

as it is increased.

Fig. 16. reveals the state of nondimensional rate of heat transfer against the Prandtl number ( $Pr$ ) for different values of dimensionless temperature jump parameter ( $h_2$ ). It is evident that, for increasing dimensionless temperature jump parameter the nondimensional rate of heat transfer gets reduced significantly. For increasing Prandtl number, the non dimensional heat transfer rate gets increased effectively for  $h_2 = 0$  than  $h_2 > 0$ .

Physically stretching surfaces are often encountered in many industrial manufacturing processes like glass blowing, liquid metal production, metal extrusion, glass fiber production and polymer extrusion. Stretching surfaces practically need not to be flat; it may have some thickness variations in which the rate of cooling of the product is vital. Especially in glass blowing process due to the smoothness of the surface, the velocity may slip over the surface and during this process random heating is done which may give some rise to temperature jump at the surface. From the results it is evident

that increasing magnetic field strength has the tendency to suppress the flow motion which reduces its capacity to drive away the temperature from the sheet. Similarly, increase in temperature jump parameter increases the thermal accommodation which leads to reduction of the thermal diffusion towards the flow. Hence it is clear that both magnetic field strength and temperature jump make the heat transfer process slow. Since the rate of cooling has significant effects on the glass blowing process, both magnetic field strength and temperature jump may play individual vital role in achieving best quality of the final products.

## 6. CONCLUSION

The problem of steady, two dimensional, non-linear, laminar hydromagnetic flow of an incompressible, viscous and electrically conducting fluid over a stretching sheet with variable thickness in slip flow regime has been analyzed. A parametric study on dimensionless velocity, temperature, skin friction coefficient, heat transfer rate are carried out. In the absence of magnetic interaction parameter ( $M^2 = 0$ ) and nondimensional temperature jump parameter ( $h_2 = 0$ ), the numerical values of  $-F''(0)$  are found to be in excellent agreement with that of Khader and Megahed (2013). From the results of the present investigation, following conclusions are drawn:

- Dimensionless velocity gets accelerated by the increasing velocity power index whereas it gets decelerated by the Lorentz force of increased magnetic field strength and for increasing wall thickness. Dimensionless velocity slip parameter has the tenancy to both increase and decrease the velocity distribution.
- The magnetic field, velocity power index and dimensionless velocity slip parameter has the influence to enhance the temperature distribution, whereas the wall thickness parameter, dimensionless temperature jump parameter and Prandtl number has different effects to suppress the dimensionless temperature distribution.
- Dimensionless skin friction coefficient has decreased for increasing magnetic field, velocity power index parameter with velocity slip ( $h_1 > 0$ ) and wall thickness. It gets increased for increasing values of dimensionless temperature jump parameter and velocity power index parameter without the velocity slip ( $h_1 = 0$ ).
- Wall thickness parameter, velocity power index parameter and the Prandtl number especially for  $h_2 = 0$  than  $h_2 > 0$  are to enhance the non dimensional rate of heat transfer. The magnetic field strength, dimensionless velocity slip parameter and dimensionless temperature jump parameter pulls down the non dimensional heat transfer rate.
- Thickening of the boundary layer occurs for increasing values of velocity power index, whereas it get thinner for increase in magnetic field strength, wall thickness parameter and dimensionless velocity slip parameter.
- Thermal boundary layer is enriched by magnetic field, velocity power index parameter and dimensionless velocity slip parameter. Thinner thermal boundary layer is obtained for increasing wall thickness, Prandtl number and dimensionless temperature jump parameter.

## ACKNOWLEDGMENT

Heartful thanks from the Second author to the Department of Science & Technology, Government of India for providing the Project Fellowship through Promotion of University Research and Scientific Excellence (DST-PURSE) Program during this work.

## REFERENCES

- Altan, T., S. Oh and H. Gegel (1979). *Metal forming fundamentals and applications*. Ohio: American society for metals.
- Andersson, H. (2002). Slip flow past a stretching surface. *Acta Mechanica* 158, 121–125.
- Anjali, D. S. and B. Ganga (2010). Dissipation effects on mhd nonlinear flow and heat transfer past a porous surface with prescribed heat flux. *Journal of Applied Fluid Mechanics (JAFM)* 3(1), 1.
- Anjali, D. S. and M. Prakash (2014). Steady nonlinear hydromagnetic flow over a stretching sheet with variable thickness and variable surface temperature. *Journal of the Korean Society for Industrial and Applied Mathematics* 18, 245–256.
- Anjali Devi, S. and M. Thiyagarajan (2006). Steady nonlinear hydromagnetic flow and heat transfer over a stretching surface of variable temperature. *Heat and Mass Transfer* 42(8), 671–677.

- Behrouz, R., M. S. Tauseef and Y. Ahmet (2011). Solution to the mhd flow over a non-linear stretching sheet by homotopy perturbation method. *SCIENCE CHINA Physics, Mechanics & Astronomy* 54, 342–345.
- Chakrabarti and A. Gupta (1979). Hydro-magnetic flow and heat transfer over a stretching sheet. *Quarterly Journal of Mechanics and Applied Mathematics* 37, 73–78.
- Fang, T., J. Zhang and Y. Zhong (2012). Boundary layer flow over a stretching sheet with variable thickness. *Applied Mathematics and Computation* 218, 7241–7252.
- Fisher, E. (1976). *Extrusion of plastics*. New York: Wiley.
- GadelHak, M. (1999). The fluid mechanics of microdevices - the freeman scholar lecture. *Journal of Fluid engineering* 121, 5–33.
- Karwe, M. and Y. Jaluria (1991). Numerical simulation of thermal transport associated with a continuously moving flat sheet in materials processing. *ASME Journal of Heat Transfer* 113, 612–619.
- Khader, M. and A. M. Megahed (2013). Numerical solution for boundary layer flow due to a nonlinearly stretching sheet with variable thickness and slip velocity. *The European Physical Journal Plus* 128, 100.
- Lee, L. (1967). Boundary layer over a thin needle. *Physics of fluids* 10, 822–828.
- Mukhopadhyay, S. (2013). Slip effects on mhd boundary layer flow over an exponentially stretching sheet with suction/blowing and thermal radiation. *Ain Shams Engineering Journal* 4(3), 485 – 491.
- Nachtsheim, P. R. and P. Swigert (1965, October). Satisfaction of asymptotic boundary conditions in numerical solution of systems of nonlinear equations of boundary-layer type. In *NASA Technical Note, NASA TN D-3004*, Washington, D. C, USA.
- Navier, C. (1827). Sur les lois du mouvement des liquides. *Mem. Acad. R. Sci. Inst. Fr* 6, 389–440.
- Sparrow, E. and R. Cess (1961). The effect of a magnetic field on free convection heat transfer. *International Journal of Heat and Mass Transfer* 3, 267–2741.
- Sweesy, M. W., J. L. Holland and K. W. Smith (2004). Electromagnetic interference in cardiac rhythm management devices. *AACN Clinical Issues: Advanced Practice in Acute & Critical Care* 15, 391–403.
- Wang, C. (2009). Analysis of viscous flow due to a stretching sheet with surface slip and suction. *Nonlinear Analysis: Real World Applications* 10, 375–380.
- Yazdi, M., S. Abdullah, I. Hashim and K. Sopian (2011). Slip mhd liquid flow and heat transfer over non-linear permeable stretching surface with chemical reaction. *Journal of Combinatorial Theory* 54, 3214–3225.